SAR COMPLIANCE TESTING OF PROXIM EUROPE B.V. MODEL 8460-05 CARDBUS CARD (FCC ID# HZB-8460) INSERTED INTO A LAPTOP COMPUTER

December 23, 2002

Submitted to: Mr. Mark Koop
Proxim Europe B.V.
Zadelstede 1-10 3431 JZ Nieuwegein
The Netherlands

Submitted by: Om P. Gandhi
Professor of Electrical and Computer Engineering
University of Utah
50 S Central Campus Dr., Rm. 3280
Salt Lake City, UT 84112-9206

SAR COMPLIANCE TESTING OF PROXIM EUROPE B.V. MODEL 8460-05 CARDBUS CARD (FCC ID# HZB-8460) INSERTED INTO A LAPTOP COMPUTER

I. Introduction

The U.S. Federal Communications Commission (FCC) has adopted limits of human exposure to RF emissions from mobile and portable devices that are regulated by the FCC [1]. The FCC has also issued Supplement C (Edition 97-01) to OET Bulletin 65 [2] and a more recent version of the same [3] defining both the measurement and the computational procedures that should be followed for evaluating compliance of mobile and portable devices with FCC limits for human exposure to radiofrequency emissions.

We have used the measurement procedure for SAR compliance testing of the Proxim Europe B.V. Model 8460-05 Cardbus Card inserted into the laptop computer. A photograph of the unit with the Cardbus Card inserted into the laptop computer is given in Fig. 1. A picture of the Cardbus Card placed on the laptop is given in Fig. 2. The Proxim Europe B.V. Model 8460-05 Cardbus Card operates over the frequency band 5.18 to 5.825 GHz in base or turbo modes with average conducted power levels as high as 20.3 dBm (107.2 mW).

For SAR measurements, two configurations of the wireless PC relative to the experimental phantom have been used:

a. Since the wireless PC may possibly be placed on a user's lap where the RF antennas would be the closest to the body, a planar phantom model with inside dimensions 12" x 16.5" (30.5 x 41.9 cm) and a base thickness of 2.0 ± 0.2 mm (recommended in [3]) was used for SAR measurements and the wireless PC card mounted in a portable computer (as in Fig. 1) pressed against the bottom of this phantom (see Fig. 5).

b. For a bystander, the "end-on" SAR value is obtained for the PC and the card edge at 90° to the flat phantom with a spacing of 0 cm (see Fig. 6). The SARs measured for the end-on configuration of the PC Card were extremely low close to the noise level for the FCC-recommended spacing of 2.5 cm, hence the PC Card edge in contact with the base of the planar phantom was used instead for the SAR measurements given in Figs. 15 a-d and Tables 7-10, respectively.

II. The SAR Measurement System

The University of Utah SAR Measurement System has been described in peer-reviewed literature [Ref. 4 -- attached here as Appendix A]. A photograph of the SAR Measurement System is given in Fig. 3. This SAR Measurement System uses a computer-controlled 3-D stepper motor system (Arrick Robotics MD-2A). A triaxial Narda Model 8021 E-field probe is used to determine the internal electric fields. The positioning repeatability of the stepper motor system moving the E-field probe is within ±0.1 mm. Outputs from the three channels of the E-field probe are dc voltages, the sum of which is proportional to the square of the internal electric fields $\left(|E_i|^2\right)$ from which the SAR can be obtained from the equation SAR = $\sigma\left(|E_i|^2\right)/\rho$, where σ and ρ are the conductivity and mass density of the tissue-simulant materials, respectively [5]. The dc voltages for the three channels of the E-field probe are read by three HP 34401A multimeters and sent to the computer via an HPIB interface. The setup is carefully grounded and shielded to reduce the noise due to the electromagnetic interference (EMI). A cutout in a wooden table of dimensions 38.1 × 21.6 cm allows placement of a plastic holder (shown in Fig. 4) on which the laptop computer with the Cardbus Card (see Fig. 1) is supported. The plastic holder can be moved up or down so that the base of the PC is pressed against the base of the flat phantom for determination of SAR for above-lap position (see Fig. 5). Similarly, for the "end-on" SAR determination, the laptop computer with the Proxim Europe B.V. Cardbus Card is mounted sideways on the plastic holder and moved up so that the end of the Cardbus Card is touching the base of the flat phantom (see Fig. 6).

The Flat Phantom

As recommended in Supplement C Edition 01-01 to OET Bulletin 65 [3], a planar phantom model with inside dimensions 12" × 16.5" (30.5 × 41.9 cm) and base thickness

2.0 ± 0.2 mm was used for SAR measurements (see Figs. 5, 6). As seen both in Figs. 5 and 6, a one-inch thick Styrofoam block was used under the base of the phantom to prevent bending of the 2 mm thin base.

III. Calibration of the E-Field Probe

The IEEE Draft Standard P1528 [4] suggests a recommended procedure for probe calibration (see Section 4.4.1 of [4]) for frequencies above 800 MHz where waveguide size is manageable. Calibration using a rectangular waveguide is recommended. As in some previously reported SAR measurements at 6 GHz [5], we have calibrated the Narda Model 8021 Miniature Broadband Electric Field Probe of tip diameter 4 mm (internal dipole dimensions on the order of 2.5 mm) using a rectangular waveguide WR 159 (of internal dimensions 1.59 x 0.795 inches) that was filled with the tissue-simulant fluid of composition given in Section V. The triaxial (3 dipole) E-field probe shown in Fig. 7 was originally developed by Howard Bassen and colleagues of FDA and has been manufactured under license by Narda Microwave Corporation, Hauppage, New York. The probe is described in detail in references 6 and 7. It uses three orthogonal pick up dipoles each of length about 2.5 mm offset from the tip by 3 mm, each with its own leadless zero voltage Schottky barrier diode operating in the square law region. The sum of the three diode outputs read by three microvoltmeters [8] gives an output proportional to E^2. By rotating the probe around its axis, the isotropy of the probe was measured to be less than ± 0.23 dB and the deviation of the probe from the square law behavior was less than ± 3%.

As suggested in the Draft Standard P1528, the waveguide (WR 159) filled with the tissue-simulant fluid was maintained vertically. From microwave field theory [see e.g. ref. 9], the transverse field distribution in the liquid corresponds to the fundamental mode (TE_{10}) with an exponential decay in the vertical direction (z-axis). The liquid level was 15 cm deep which is deep enough to guarantee that reflections from the top liquid surface do not affect the calibration. By comparing the square of the decaying electric fields expected in the tissue from the analytical expressions for the TE_{10} mode of the rectangular waveguide, we obtained a calibration factor of 2.98 (mW/kg)/μV with a variability of less than ±2% for measurement frequencies of 5.2, 5.3, 5.7 and 5.8 GHz, respectively. This is no doubt due to a fairly limited frequency band of only 0.6 GHz out of a recommended bandwidth of 2.2 GHz for the TE_{10} mode for the WR159 waveguide (recommended band of 4.9-7.1 GHz -- see e.g. ref. 9).

The data for the calibration of the E-field probe closest to the SAR tests given here was December 18, 2002.

IV. SAR System Verification

Since we do not have a dipole for the 5 GHz band, a half wave dipole at 1900 MHz was used instead for SAR system verification. This dipole of length 76.0 mm and diameter 1.5 mm and h = 39.5 mm is shown in Fig. 8. As recommended in OET65 Supplement C [3], we used a spacing of 10 mm from the dipole to the tissue-simulant fluid composed of 40.4% water, 58.0% sugar, 0.5% salt (NaCl), 1% HEC, and 0.1% bactericide. The microwave circuit arrangement used for system verification is sketched in Fig. 9. The dielectric properties for this body-simulant fluid were measured using the Hewlett Packard (HP) Model 85070 B Dielectric Probe (rated frequency band 200 MHz to 20 GHz in conjunction with HP Model 8720C Network Analyzer (50 MHz-20 GHz) using a procedure detailed in Section V. The measured dielectric parameters of the body-simulant fluid at 1900 MHz are $\varepsilon_r = 53.1 \pm 1.3$ and $\sigma = 1.44 \pm 0.09$ S/m. The measured properties are close to the values of $\varepsilon_r = 54.0$ and $\sigma = 1.45$ S/m given in OET Supplement C [3].

The two measured SAR distributions for the peak 1-g SAR region using this system verification dipole for each day of SAR measurements December 21, 22, 2002 are given in Appendix B. Also given in Appendix B are the dipole SAR plots for each date of device testing. The two peak 1-g SARs are 36.001 and 36.165 W/kg which is a variability of only 1.0%. Furthermore, both of the measured 1-g SARs are in excellent agreement with the FDTDcalculated 1-g SAR of 35.8 W/kg for this dipole. Also as expected, the measured SAR plots are quite symmetric.

V. Tissue Simulant Fluid for the Frequency Band 5.2 to 5.8 GHz

In OET 65 Supplement C [3], the dielectric parameters suggested for body phantom are given only for 3000 and 5800 MHz. These are listed in Table 1 here. Using linear interpolation, we can obtain the dielectric parameters to use for the frequency band between 5.2 to 5.8 GHz. The desired dielectric properties thus obtained are also given in Table 1. From Table 1, it can be noticed that the desired dielectric constant ε_r varies from 48.2 to 49.0 which is a variation of less than ± 1% from the average value of 48.6 for this band. Also the conductivity σ varies linearly with frequency from 5.3 to 6.00 S/m. For the SAR measurements given in this report, we have used a tissue-simulant fluid developed at the University of Utah which consists of 68.0% water, 31.0% sugar and 1% HEC. For this composition, we have measured the dielectric properties using a Hewlett Packard (HP) Model 85070B Dielectric Probe in conjunction with HP Model 8720C Network Analyzer (50 MHz-20 GHz). The measured dielectric properties at a mid band frequency of 5.30 GHz are as follows: $\varepsilon_r = 48.5 \pm 1.7$ and $\sigma = 5.40 \pm 0.08$ S/m. From Table 1, we obtain the desired dielectric properties to simulate the body tissue at the midband frequency of 5.30 GHz to be $\varepsilon_r = 48.9$ and $\sigma = 5.42$ S/m. Thus, the measured properties for the body-simulant fluid are close to the desired values. Also as expected, the conductivity of this fluid varies linearly with frequency rising to 6.03 ± 0.09 S/m at 5.8 GHz, while the dielectric constant ε_r is nearly the same as the measured value at 5.3 GHz.

The procedure is as follows: The HP Model 95070B Dielectric Probe (see Fig. 10) is an open-circuited transmission-line (coaxial line) probe similar to that described in Section B.1.2 of the Draft IEEE Standard 1528 [4]. The theory of the open-circuited coaxial line method has been described in scientific literature [10-12]. We have previously used this method in determining the dielectric properties of tissue-simulant materials at 6 GHz [5]. In this method, the complex reflection coefficient Γ^* measured for the open end of the coaxial line can be used to calculate the complex permittivity ε^* from the following equation [5]

$$\varepsilon^* = \frac{1-\Gamma^*}{j\omega Z_o C_o\left(1+\Gamma^*\right)} - \frac{C_f}{C_o} \qquad (1)$$

where Z_o is the characteristic impedance (50 Ω) for the coaxial line, C_o is the capacitance when the line is in air and C_f is the capacitance that accounts for the fringing fields in the dielectric of the coaxial line.

For the HP85070B Dielectric Probe with diameters of the outer and inner conductors 2b = 3.00 mm and 2a = 0.912 mm, respectively, the following capacitances were obtained using deionized water and methanol as the calibration fluids. The following capacitances were obtained:

$$C_o = 0.022 \text{ pF}$$

$$C_f = 0.005 \text{ pF}$$

Using the network analyzer HP8720C, we measured the reflection coefficient Γ^* for the open end of the coaxial line that was submerged in the tissue-simulant fluid. Using Eq. 1, the complex permittivity of the fluid was measured at various frequencies 5.2-5.8 GHz. From the imaginary part of the complex permittivity Im(ε^*), we can obtain the conductivity σ from the relationship

$$\sigma = \frac{\mathrm{Im}(\varepsilon^*)}{\omega\varepsilon_o} \qquad (2)$$

VI. The Measured SAR Distributions

Using a Hewlett Packard Model 436A Power Meter, the maximum power output of the Proxim Europe B.V. Model 8460-05 Cardbus Card was measured for both base and turbo modes at a number of frequencies through the coaxial connector provided for this purpose on the Cardbus Card (see Figs. 11 and 12). The RF power output thus measured is given in Table 2. Recognizing that the power outputs were the highest at 5.26 and 5.785 GHz for the base mode and at 5.29 and 5.80 GHz for the turbo mode (see Table 2), the SAR measurements were conducted for these four power output conditions of the Proxim Europe B.V. Cardbus Card. Also as recommended in Supplement C, Edition 01-01 [3], the conducted power was measured before and after each SAR measurement and found to be within ±0.1 dB (±2.5%) of the values given in Table 2.

The highest SAR region for each of the measurement frequencies was identified in the first instance by using a coarser sampling with a step size of 8.0 mm over three overlapping areas for a total scan area of 8.0 × 9.6 cm. The data thus obtained is resolved into a 4 x 4 times larger grid i.e. a grid involving 40 x 28 points by linear interpolation using a 2 mm step size. After thus identifying the region of the highest SAR, the SAR distribution was then measured with a resolution of 2 mm in order to obtain the peak 1 cm^3 or 1-g SAR. The SAR measurements are performed at 4, 6, 8, 10, 12 mm height from the bottom surface of the body-simulant fluid. The SARs thus measured were extrapolated using a second-order least-square fit to the measured data to obtain values at 1, 3, 5, 7 and 9 mm height and used to obtain 1-g SARs. The uncertainty analysis of the University of Utah SAR measurement system is given in Appendix C. The combined standard uncertainty is ± 8.3%.

The coarse scans for the four measurements for the Above-lap position are shown in Fig. 13a-d, respectively. In these figures, the two axes are marked in units of the step size of 8 mm. The highest SAR region shown in maroon color is immediately above the region of the radiating antenna as illustrated in Fig. 14. Given in Tables 3-7 are the SAR distributions for the peak SAR region of volume 10 ×10 ×mm for which the coarse scans are given in Figs. 13a-d, respectively. The SARs are given for xy planes at heights z of 1, 3, 5, 7, and 9 mm for the Proxim Europe B.V. Cardbus Card inserted in the laptop computer which is pressed against the bottom of the flat phantom. The individual SAR values for this grid of 5 × 5 × 5 or 125 points are averaged to obtain peak 1-g SAR values (for a volume of 1 cm^3). The temperature variation of the tissue-simulant fluid measured with a Bailey Instruments Model BAT 8 Temperature Probe over the 80-minute period needed for measurements at the four frequencies was $23.7 \pm 0.2^{\circ}C$.

The coarse scans measurements for the four measurements for the End-on position are shown in Fig. 15a-d, respectively. The corresponding SAR distributions for the peak 1-g SAR are given in Tables 7-10, respectively. The z-axis scan plots taken at the highest SAR locations for each set of tests are given in Fig. 16 and 17, respectively.

For the measurements in Tables 3-6, the separation between the Proxim Europe B.V. Cardbus Card and the bottom of the experimental phantom is on the order of 1 cm. For the "end-on" position, the SARs for an FCC-recommended separation of 2.5 cm to the bottom of the flat phantom were extremely low close to the noise level. Therefore, the PC Card edge at 90° in contact with the base of the phantom was used instead for the SAR measurements given in Figs. 15a-d and Tables 7-10, respectively. The peak 1-g SARs for the various configurations of the Cardbus Card are summarized in Table 11. All of the measured 1-g SARs are less than the FCC 96-326 guideline of 1.6 W/kg.

VII. Comparison of the Data with FCC 96-326 Guidelines

According to the FCC 96-326 Guideline [1], the peak SAR for any 1-g of tissue should not exceed 1.6 W/kg. For the Proxim Europe B.V. Model 8460-05 Cardbus Card, the measured peak 1-g SARs vary from 0.19 to 0.98 W/kg which are smaller than 1.6 W/kg.

REFERENCES

1. Federal Communications Commission, "Guidelines for Evaluating the Environmental Effects of Radiofrequency Radiation," FCC 96-326, August 1, 1996.

2. K. Chan, R. F. Cleveland, Jr., and D. L. Means, "Evaluating Compliance With FCC Guidelines for Human Exposure to Radiofrequency Electromagnetic Fields," Supplement C (Edition 97-01) to OET Bulletin 65, December, 1997. Available from Office of Engineering and Technology, Federal Communications Commission, Washington D.C., 20554.

3. Federal Communications Commission "Supplement C Edition 01-01 to OET Bulletin 65 Edition 97-01" June 2001.

4. IEEE Draft Standard P1528, "Recommended Practice for Determining the Peak Spatial-Average Specific Absorption Rate (SAR) in the Human Body Due to Wireless Communication Devices: Experimental Techniques," Draft CBD1.0, April 4, 2002 (IEEE Standards Coordinating Committee 34).

5. O. P. Gandhi and J-Y. Chen, "Electromagnetic Absorption in the Human Head from Experimental 6-GHz Handheld Transceivers," *IEEE Transactions on Electromagnetic Compatibility*, Vol. 39(4), pp. 547-558, 1995.

6. H. Bassen. M. Swicord, and J. Abita, "A Miniature Broadband Electric Field Probe," Ann. New York Academy of Sciences, Vol. 247, pp. 481-493, 1974.

7. H. Bassen and T. Babij, "Experimental Techniques and Instrumentation," Chapter 7 in *Biological Effects and Medical Applications of Electromagnetic Energy*, O. P. Gandhi, Editor, Prentice Hall Inc., Englewood Cliffs, NJ, 1990.

8. Q. Yu, O. P. Gandhi, M. Aronsson, and D. Wu, "An Automated SAR Measurement System for Compliance Testing of Personal Wireless Devices," *IEEE Transactions on Electromagnetic Compatibility,* Vol. 41(3), pp. 234-245, August 1999 (attached as Appendix A).

9. O. P. Gandhi, *Microwave Engineering and Applications,* Pergamon Press, New York, 1981.

10. T. W. Athey, M. A. Stuchly, and S. S. Stuchly, "Measurement of Radiofrequency Permittivity of Biological Tissues with an Open-Circuited Coaxial Line - Part I," *IEEE Transactions on Microwave Theory and Techniques*, Vol. MTT-30, pp. 82-86, 1982.

11. M. A. Stuchly, T. W. Athey, G. M. Samaras, and G. E. Taylor, "Measurement of Radiofrequency Permittivity of Biological Tissues with an Open-Circuited Coaxial Line - Part II - Experimental Results," *IEEE Transactions on Microwave Theory and Techniques*, Vol. MTT-30, pp. 87-92, 1982.

12. C. L. Pournaropoulos and D. K. Misra, "The Coaxial Aperture Electromagnetic Sensor and Its Application for Material Characterization," *Measurement Science and Technology*, Vol. 8, pp. 1191-1202, 1997.

Table 1. Dielectric parameters for body phantom for the frequency band 5.2 to 5.8 GHz [3].

Frequency GHz	ε_r	σ S/m	Reference
3.0	52.0	2.73	Ref. 3
5.8	48.2	6.00	Ref. 3
5.2	49.0	5.30	Interpolated
5.3	48.9	5.42	Interpolated
5.4	48.7	5.53	Interpolated
5.6	48.5	5.77	Interpolated
5.7	48.3	5.88	Interpolated

Table 2. Average conducted RF power outputs measured at various frequencies for the Proxim Europe B.V. Model 8460-05 Cardbus Card for base and turbo modes.

Frequency GHz	Average Power dBm
Base Mode	
5.18	15.11
5.26	19.00
5.32	14.30
5.745	18.9
5.785	19.3
5.825	19.2
Turbo Mode	
5.21	16.21
5.25	16.02
5.29	17.62
5.760	20.3
5.800	20.3

Table 3. **Above-lap position.** The SARs measured for the Proxim Europe B.V. 8460-05 Cardbus Card inserted into a laptop computer for the base mode at 5.26 GHz.

1-g SAR = 0.702 W/kg

a. At depth of 1 mm

1.166	1.293	1.339	1.358	1.296
1.257	1.364	1.427	1.440	1.389
1.306	1.406	1.477	1.458	1.421
1.261	1.380	1.424	1.442	1.349
1.240	1.334	1.383	1.385	1.294

b. At depth of 3 mm

0.822	0.899	0.931	0.940	0.904
0.874	0.943	0.990	0.998	0.962
0.902	0.975	1.014	1.013	0.985
0.884	0.962	0.992	0.996	0.942
0.856	0.930	0.964	0.963	0.910

c. At depth of 5 mm

0.550	0.588	0.609	0.611	0.595
0.572	0.610	0.645	0.647	0.625
0.585	0.635	0.650	0.661	0.641
0.585	0.630	0.650	0.645	0.621
0.555	0.611	0.632	0.629	0.604

d. At depth of 7 mm

0.347	0.359	0.371	0.369	0.368
0.351	0.365	0.392	0.389	0.379
0.354	0.386	0.385	0.401	0.389
0.363	0.385	0.397	0.389	0.384
0.337	0.375	0.387	0.384	0.378

e. At depth of 9 mm

0.215	0.212	0.219	0.216	0.224
0.210	0.207	0.231	0.223	0.223
0.208	0.227	0.218	0.235	0.229
0.220	0.226	0.233	0.226	0.233
0.203	0.223	0.231	0.227	0.231

Table 4. **Above-lap position.** The SARs measured for the Proxim Europe B.V. 8460-05 Cardbus Card inserted into a laptop computer for the base mode at 5.785 GHz.

1-g SAR = 0.843 W/kg

a. At depth of 1 mm

1.516	1.570	1.630	1.669	1.602
1.633	1.752	1.796	1.791	1.687
1.741	1.815	1.956	1.894	1.767
1.780	1.884	1.905	1.878	1.714
1.628	1.728	1.817	1.736	1.604

b. At depth of 3 mm

1.024	1.066	1.099	1.110	1.072
1.100	1.167	1.213	1.198	1.134
1.184	1.228	1.281	1.258	1.186
1.195	1.247	1.268	1.247	1.163
1.085	1.164	1.224	1.189	1.130

c. At depth of 5 mm

0.636	0.667	0.681	0.674	0.656
0.680	0.710	0.753	0.734	0.700
0.745	0.764	0.756	0.760	0.728
0.735	0.749	0.768	0.754	0.725
0.661	0.721	0.760	0.759	0.754

d. At depth of 7 mm

0.351	0.373	0.376	0.360	0.355
0.373	0.379	0.415	0.399	0.383
0.424	0.421	0.382	0.400	0.393
0.400	0.391	0.406	0.398	0.403
0.357	0.398	0.425	0.444	0.476

e. At depth of 9 mm

0.170	0.184	0.185	0.168	0.169
0.179	0.175	0.199	0.192	0.183
0.220	0.201	0.157	0.178	0.183
0.191	0.172	0.181	0.180	0.195
0.172	0.197	0.218	0.246	0.295

Table 5. **Above-lap position.** The SARs measured for the Proxim Europe B.V. 8460-05 Cardbus Card inserted into a laptop computer for the turbo mode at 5.29 GHz.

1-g SAR = 0.547 W/kg

a. At depth of 1 mm

1.050	1.113	1.122	1.113	1.052
1.126	1.171	1.181	1.176	1.089
1.145	1.160	1.172	1.194	1.061
1.098	1.117	1.128	1.084	1.040
1.000	1.033	1.031	0.993	0.953

b. At depth of 3 mm

0.717	0.756	0.761	0.752	0.712
0.765	0.794	0.804	0.796	0.743
0.780	0.792	0.799	0.814	0.728
0.751	0.770	0.771	0.742	0.710
0.688	0.716	0.716	0.690	0.663

c. At depth of 5 mm

0.453	0.474	0.475	0.468	0.445
0.479	0.497	0.506	0.496	0.469
0.492	0.501	0.504	0.513	0.463
0.476	0.494	0.488	0.471	0.449
0.440	0.463	0.464	0.450	0.433

d. At depth of 7 mm

0.258	0.266	0.265	0.259	0.249
0.270	0.280	0.287	0.277	0.268
0.279	0.287	0.287	0.291	0.267
0.274	0.288	0.279	0.271	0.255
0.255	0.274	0.276	0.270	0.263

e. At depth of 9 mm

0.133	0.133	0.131	0.127	0.124
0.137	0.142	0.148	0.138	0.138
0.143	0.151	0.148	0.149	0.140
0.143	0.153	0.143	0.141	0.129
0.134	0.149	0.152	0.153	0.153

Table 6. **Above-lap position.** The SARs measured for the Proxim Europe B.V. 8460-05 Cardbus Card inserted into a laptop computer for the turbo mode at 5.800 GHz.

1-g SAR = 0.984 W/kg

a. At depth of 1 mm

1.914	2.006	2.049	1.972	1.886
1.946	2.061	2.126	2.041	1.957
1.909	2.056	2.085	2.001	1.945
1.851	1.930	1.992	2.003	1.985
1.821	1.897	1.939	1.933	1.830

b. At depth of 3 mm

1.300	1.372	1.385	1.347	1.284
1.335	1.399	1.429	1.400	1.331
1.317	1.393	1.397	1.338	1.321
1.264	1.324	1.369	1.356	1.352
1.256	1.294	1.326	1.318	1.284

c. At depth of 5 mm

0.820	0.874	0.867	0.854	0.812
0.856	0.880	0.883	0.895	0.841
0.850	0.872	0.858	0.823	0.831
0.803	0.847	0.876	0.850	0.857
0.809	0.823	0.844	0.838	0.856

d. At depth of 7 mm

0.475	0.513	0.495	0.494	0.471
0.506	0.506	0.495	0.523	0.488
0.508	0.493	0.469	0.455	0.475
0.466	0.498	0.513	0.487	0.500
0.482	0.481	0.492	0.496	0.545

e. At depth of 9 mm

0.265	0.288	0.268	0.266	0.260
0.288	0.276	0.262	0.286	0.270
0.291	0.255	0.229	0.235	0.254
0.254	0.278	0.281	0.266	0.281
0.274	0.271	0.271	0.289	0.352

Table 7. **End-on position.** The SARs measured for the Proxim Europe B.V. 8460-05 Cardbus Card inserted into a laptop computer for the base mode at 5.26 GHz.

1-g SAR = 0.261W/kg

a. At depth of 1 mm

0.447	0.479	0.476	0.456	0.412
0.497	0.567	0.543	0.502	0.470
0.500	0.537	0.554	0.529	0.477
0.437	0.491	0.512	0.482	0.441
0.399	0.452	0.454	0.462	0.443

b. At depth of 3 mm

0.315	0.337	0.332	0.324	0.297
0.353	0.390	0.384	0.352	0.339
0.360	0.377	0.390	0.372	0.336
0.319	0.345	0.362	0.343	0.317
0.286	0.320	0.332	0.337	0.328

c. At depth of 5 mm

0.211	0.225	0.219	0.219	0.206
0.240	0.253	0.257	0.234	0.235
0.247	0.250	0.260	0.247	0.224
0.222	0.231	0.243	0.232	0.218
0.197	0.217	0.236	0.239	0.237

d. At depth of 7 mm

0.135	0.143	0.136	0.140	0.139
0.157	0.154	0.162	0.147	0.158
0.163	0.157	0.165	0.156	0.143
0.149	0.148	0.156	0.151	0.144
0.133	0.143	0.166	0.168	0.170

e. At depth of 9 mm

0.088	0.090	0.082	0.087	0.096
0.103	0.094	0.100	0.091	0.107
0.106	0.096	0.104	0.097	0.092
0.097	0.097	0.101	0.099	0.094
0.092	0.099	0.121	0.124	0.125

Table 8. **End-on position.** The SARs measured for the Proxim Europe B.V. 8460-05 Cardbus Card inserted into a laptop computer for the base mode at 5.785 GHz.

1-g SAR = 0.231 W/kg

a. At depth of 1 mm

0.406	0.436	0.457	0.449	0.451
0.401	0.448	0.423	0.437	0.436
0.409	0.453	0.435	0.452	0.453
0.429	0.424	0.438	0.450	0.449
0.420	0.405	0.452	0.455	0.444

b. At depth of 3 mm

0.286	0.310	0.323	0.313	0.302
0.283	0.316	0.300	0.302	0.303
0.284	0.312	0.304	0.311	0.312
0.292	0.290	0.301	0.316	0.313
0.298	0.289	0.316	0.325	0.310

c. At depth of 5 mm

0.191	0.210	0.217	0.205	0.187
0.191	0.211	0.201	0.198	0.198
0.186	0.201	0.200	0.201	0.201
0.186	0.185	0.195	0.210	0.205
0.202	0.198	0.209	0.224	0.205

d. At depth of 7 mm

0.121	0.135	0.138	0.126	0.107
0.123	0.132	0.126	0.122	0.120
0.117	0.120	0.124	0.122	0.120
0.111	0.109	0.120	0.131	0.127
0.131	0.131	0.134	0.151	0.129

e. At depth of 9 mm

0.078	0.087	0.086	0.076	0.060
0.080	0.080	0.074	0.076	0.070
0.074	0.069	0.075	0.075	0.069
0.065	0.063	0.074	0.080	0.078
0.086	0.090	0.088	0.107	0.071

Table 9. **End-on position.** The SARs measured for the Proxim Europe B.V. 8460-05 Cardbus Card inserted into a laptop computer mode for the turbo mode at 5.29 GHz.

1-g SAR = 0.190 W/kg

a. At depth of 1 mm

0.349	0.381	0.388	0.382	0.340
0.383	0.437	0.457	0.425	0.410
0.395	0.419	0.473	0.441	0.421
0.367	0.403	0.434	0.413	0.408
0.352	0.382	0.388	0.380	0.369

b. At depth of 3 mm

0.228	0.247	0.251	0.250	0.227
0.253	0.290	0.298	0.282	0.270
0.267	0.284	0.315	0.295	0.276
0.247	0.264	0.287	0.278	0.270
0.243	0.260	0.260	0.266	0.262

c. At depth of 5 mm

0.132	0.142	0.144	0.147	0.136
0.149	0.173	0.174	0.169	0.160
0.165	0.177	0.189	0.179	0.163
0.151	0.155	0.172	0.172	0.162
0.156	0.163	0.160	0.176	0.180

d. At depth of 7 mm

0.061	0.065	0.067	0.073	0.067
0.074	0.088	0.084	0.085	0.079
0.088	0.096	0.096	0.095	0.082
0.079	0.076	0.088	0.095	0.083
0.091	0.090	0.088	0.111	0.121

e. At depth of 9 mm

0.016	0.017	0.019	0.027	0.021
0.026	0.033	0.028	0.032	0.027
0.037	0.043	0.037	0.041	0.031
0.030	0.027	0.035	0.047	0.033
0.047	0.043	0.044	0.070	0.087

Table 10. **End-on position.** The SARs measured for the Proxim Europe B.V. 8460-05 Cardbus Card inserted into a laptop computer for the turbo mode at 5.800 GHz.

1-g SAR = 0.480 W/kg

a. At depth of 1 mm

0.947	0.986	0.935	0.918	0.836
0.973	0.994	0.992	0.943	0.887
0.931	0.922	0.998	0.944	0.962
1.016	0.940	0.972	0.997	0.946
0.873	0.962	0.917	0.985	0.946

b. At depth of 3 mm

0.622	0.670	0.658	0.633	0.578
0.656	0.672	0.673	0.657	0.619
0.627	0.629	0.657	0.645	0.652
0.664	0.626	0.645	0.669	0.633
0.602	0.659	0.658	0.657	0.649

c. At depth of 5 mm

0.374	0.411	0.437	0.405	0.375
0.407	0.421	0.422	0.426	0.403
0.388	0.395	0.395	0.409	0.407
0.393	0.381	0.391	0.412	0.391
0.387	0.419	0.451	0.494	0.439

d. At depth of 7 mm

0.205	0.234	0.271	0.236	0.227
0.228	0.241	0.237	0.251	0.240
0.213	0.222	0.210	0.235	0.226
0.201	0.205	0.210	0.226	0.221
0.227	0.245	0.299	0.313	0.237

e. At depth of 9 mm

0.113	0.128	0.161	0.124	0.136
0.118	0.132	0.119	0.131	0.132
0.103	0.109	0.102	0.123	0.109
0.089	0.098	0.103	0.110	0.121
0.123	0.134	0.199	0.206	0.113

Table 11. The peak 1-g SARs measured for the Proxim Europe B.V. Model 8460-05 Cardbus Card inserted into a laptop computer.

1-g SAR in W/kg

PC position relative To the flat phantom	Spacing to the bottom of the phantom	5.26 GHz base mode	5.785 GHz base mode	5.29 GHz turbo mode	5.800 GHz turbo mode
"Above-lap": bottom of PC pressed against bottom of the flat phantom	1 cm	0.702	0.843	0.547	0.984
"End-on": card edge at 90° pressed against the bottom of the flat phantom	0 cm	0.261	0.231	0.190	0.480

Fig. 1. Photograph of the Proxim Europe B.V. Model 8460-05 Cardbus Card inserted into a laptop computer.

Fig. 2. A picture of the Proxim Europe B.V. Model 8460-05 Cardbus Card placed on the laptop computer.

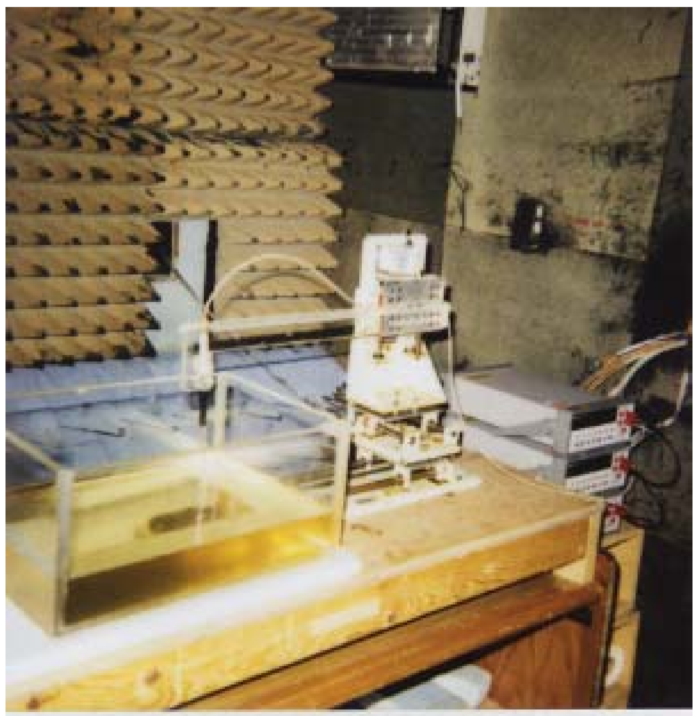

Fig. 3. Photograph of the three-dimensional stepper-motor-controlled SAR measurement system using a planar phantom (see Fig. 5 for a detailed examination of the placement of Proxim Europe B.V. Model 8460-05 Cardbus Card relative to this phantom).

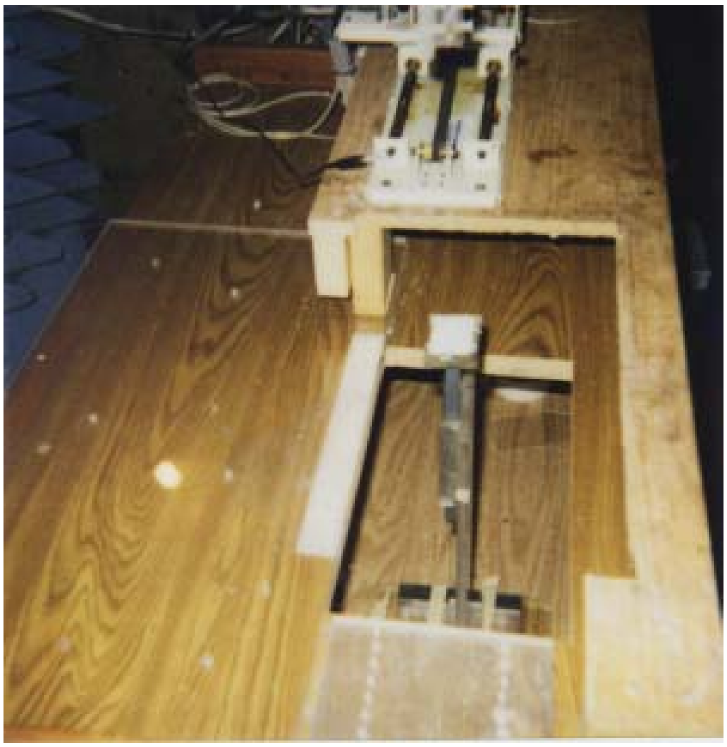

Fig. 4. The plastic holder used to support the portable computer with the Proxim Europe B.V. Model 8460-05 Cardbus Card (shown in Fig. 1).

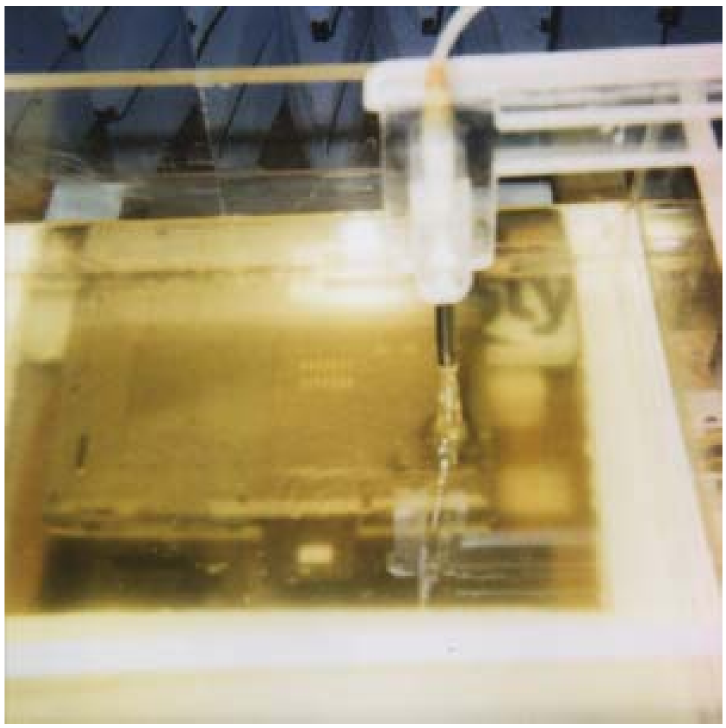

Fig. 5. Photograph of the Proxim Europe B.V. Model 8460-05 Cardbus Card inserted into a laptop computer with its bottom pressed against the bottom of the planar tissue-simulant phantom to simulate "above-lap" placement of the wireless PC. A Styrofoam block is used under the base to prevent bending of the 2 mm thin base of the phantom.

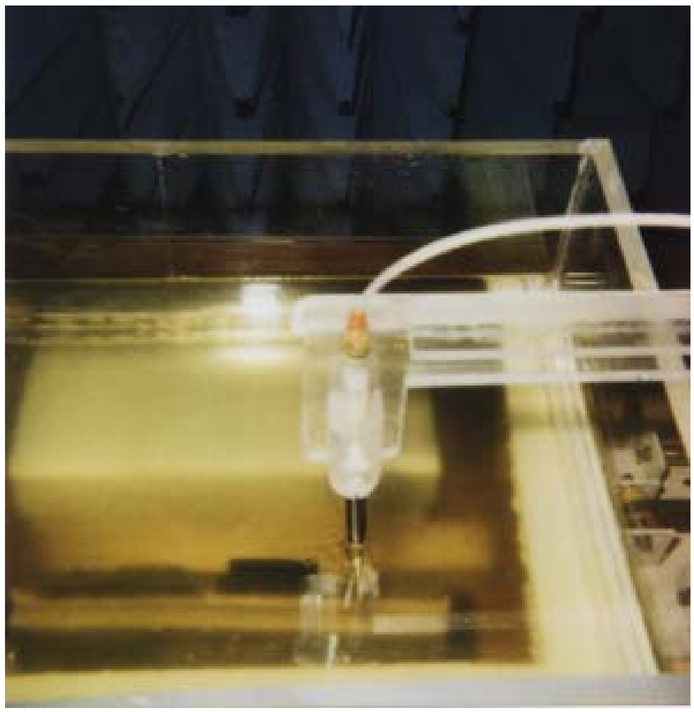

Fig. 6. Photograph of the Proxim Europe B.V. Model 8460-05 Cardbus Card inserted into a portable computer (as in Fig. 1) placed with the card edge at 90° and separated from the bottom of the phantom by 0 cm for "end-on" testing of SAR. As in Fig. 5, here too, a Styrofoam block is used under the base to prevent bending of the 2 mm thin base of the phantom.

Fig. 7. Photograph of the Narda Model 8021 Broadband Electric Field Probe used for SAR measurements.

Fig. 8. Photograph of the half-wave dipole at 1900 MHz used for system verification.

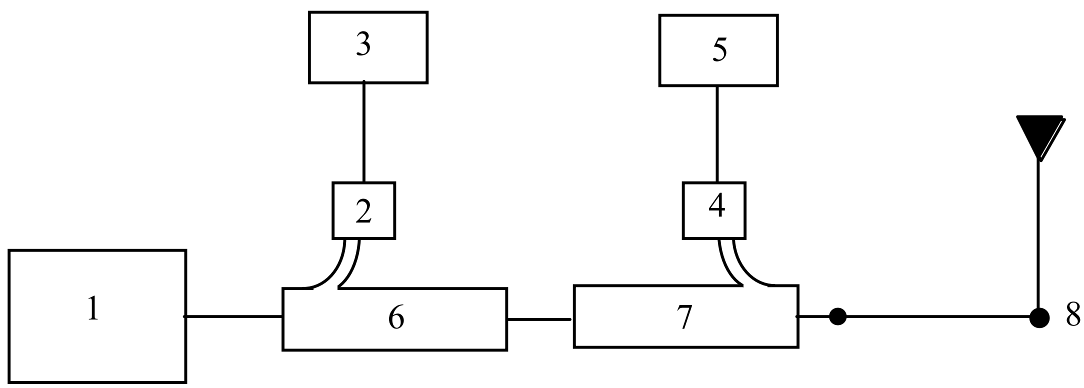

1. RF generator, MCL Model 15222 with Model 6051 plug-in (1000-2000 MHz).
2. HP Model 8481A power sensor.
3. HP Model 436A power meter.
4. HP Model 8482A power sensor.
5. HP Model 436A power meter.
6. Narda Model 3042B-30, 30 dB coaxial directional coupler.
7. Narda Model 3042-10, 10 dB coaxial directional coupler.
8. Reference dipole antenna.

Fig. 9. The microwave circuit arrangement used for SAR system verification.

Fig. 10. Photograph of the Hewlett Packard Model 85070B Dielectric Probe. This is an open-circuited coaxial line probe.

Fig. 11. Photograph of the Proxim Europe B.V. Model 8460-05 Cardbus Card with coaxial output for conducted power measurements.

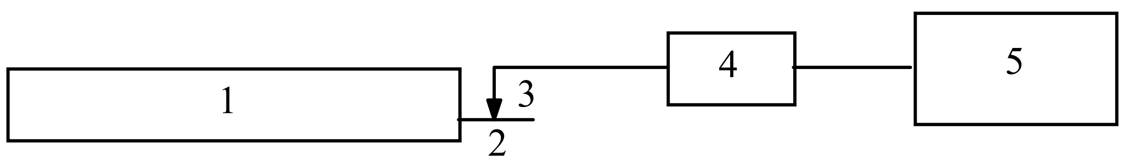

1. Laptop computer
2. Proxim Cardbus Card.
3. Coaxial output for conducted power measurements.
4. HP Model 8481A Power Sensor.
5. HP Model 436A Power Meter.

Fig. 12. The microwave circuit arrangement used for conducted power measurements for the Proxim Europe B.V. Model 8460-05 Cardbus Card.

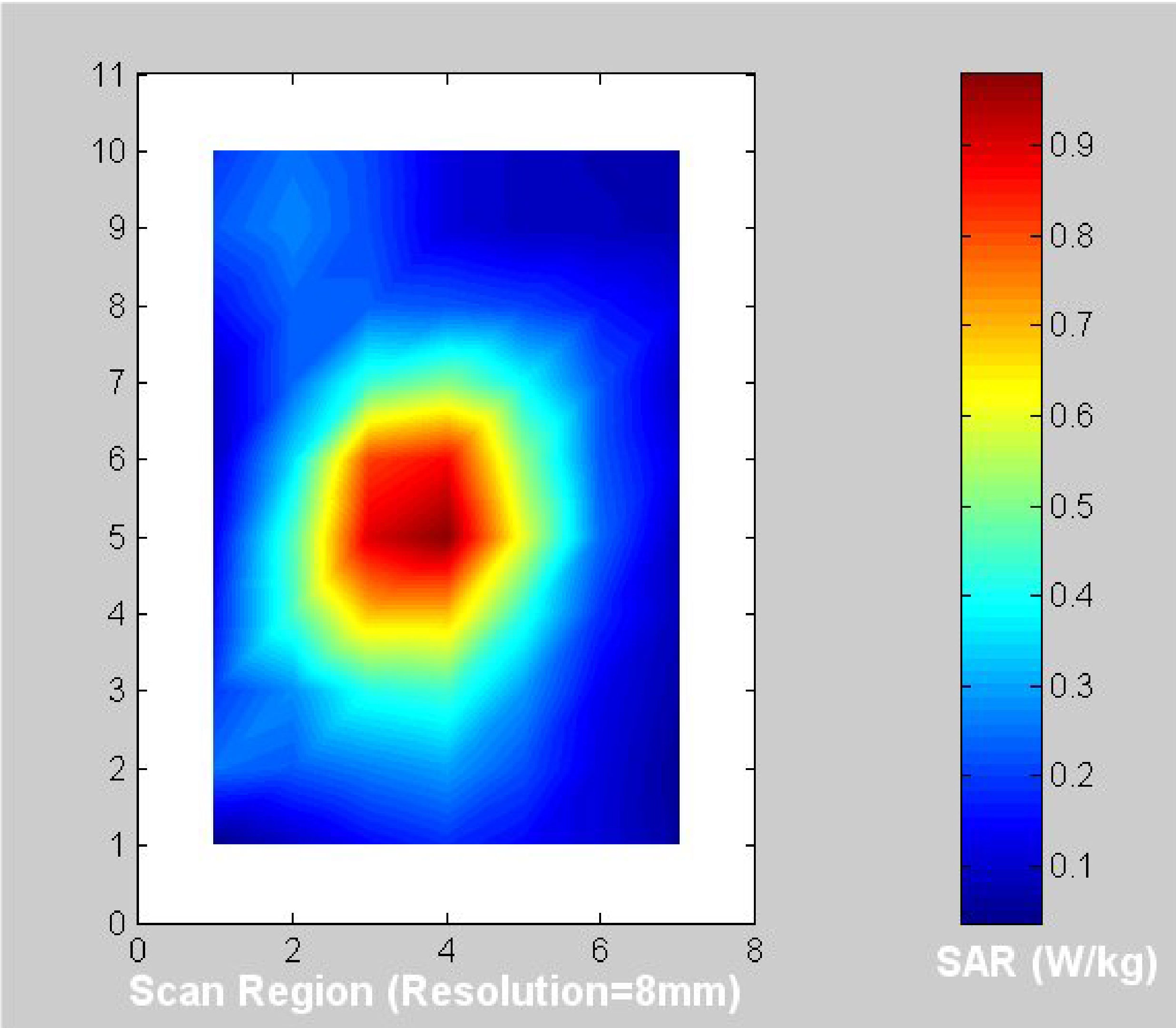

(a) 5.26 GHz base mode (see Table 3 for the peak 1-g SAR).

Fig. 13. Coarse scans for the SAR measurements for the **Above-lap position** of the Proxim Europe B.V. Model 8460-05 Cardbus Card inserted in a laptop computer.

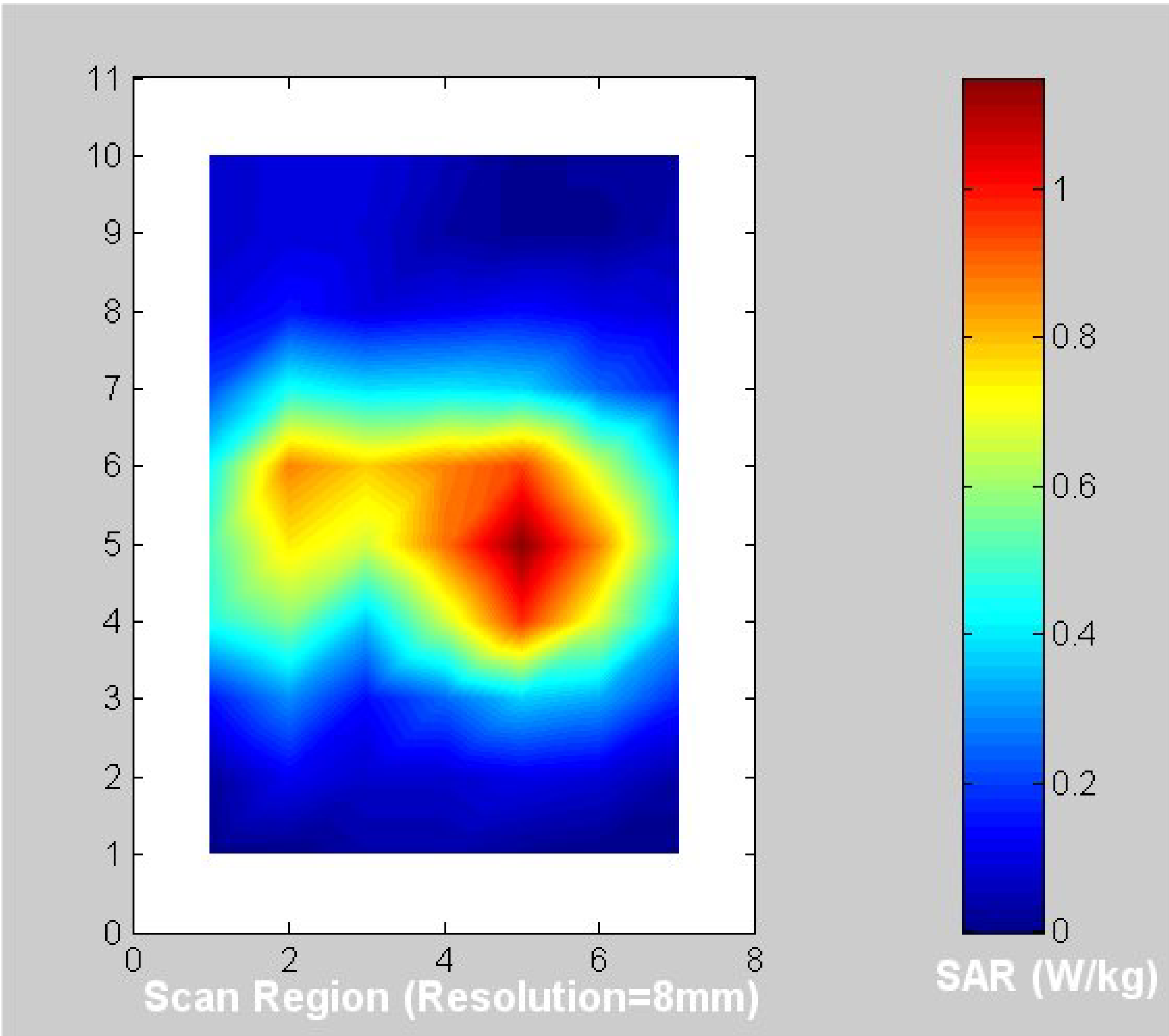

(b) 5.785 GHz base mode (see Table 4 for the peak 1-g SAR).

Fig. 13. Coarse scans for the SAR measurements for the **Above-lap position** of the Proxim Europe B.V. Model 8460-05 Cardbus Card inserted in a laptop computer.

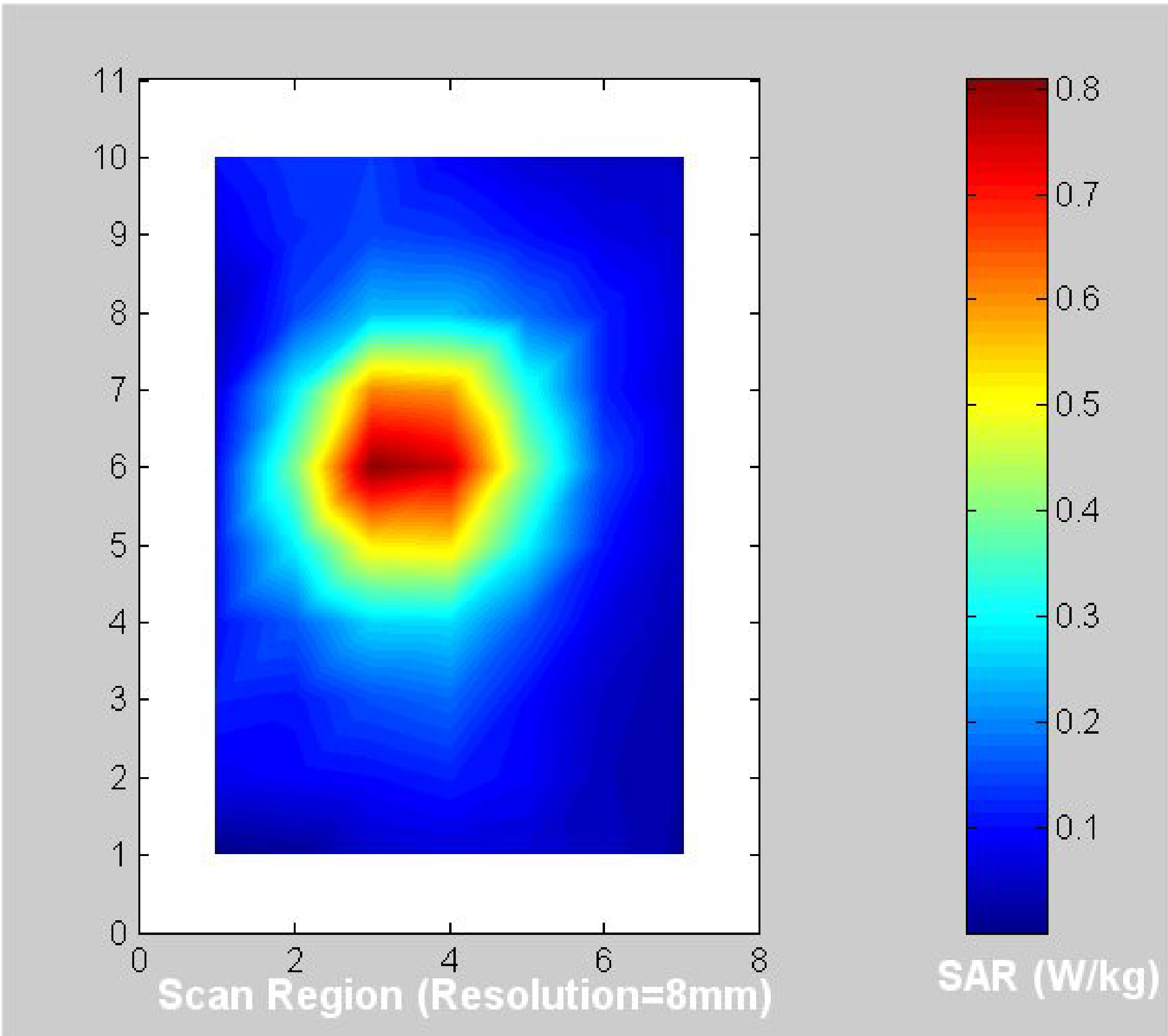

(c) 5.29 GHz turbo mode (see Table 5 for the peak 1-g SAR).

Fig. 13. Coarse scans for the SAR measurements for the **Above-lap position** of the Proxim Europe B.V. Model 8460-05 Cardbus Card inserted in a laptop computer.

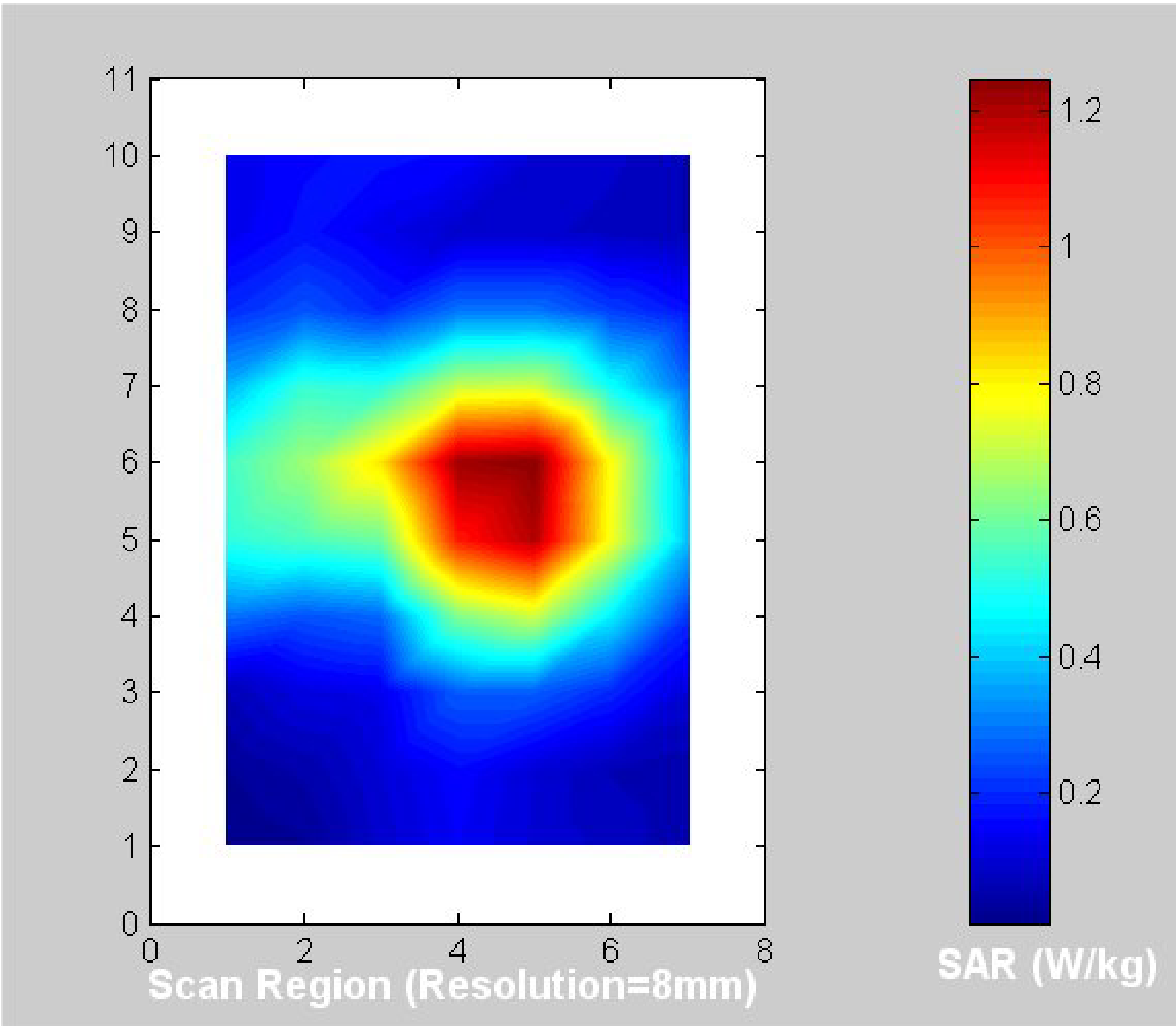

(d) 5.800 GHz turbo mode (see Table 6 for the peak 1-g SAR).

Fig. 13. Coarse scans for the SAR measurements for the **Above-lap position** of the Proxim Europe B.V. Model 8460-05 Cardbus Card inserted in a laptop computer.

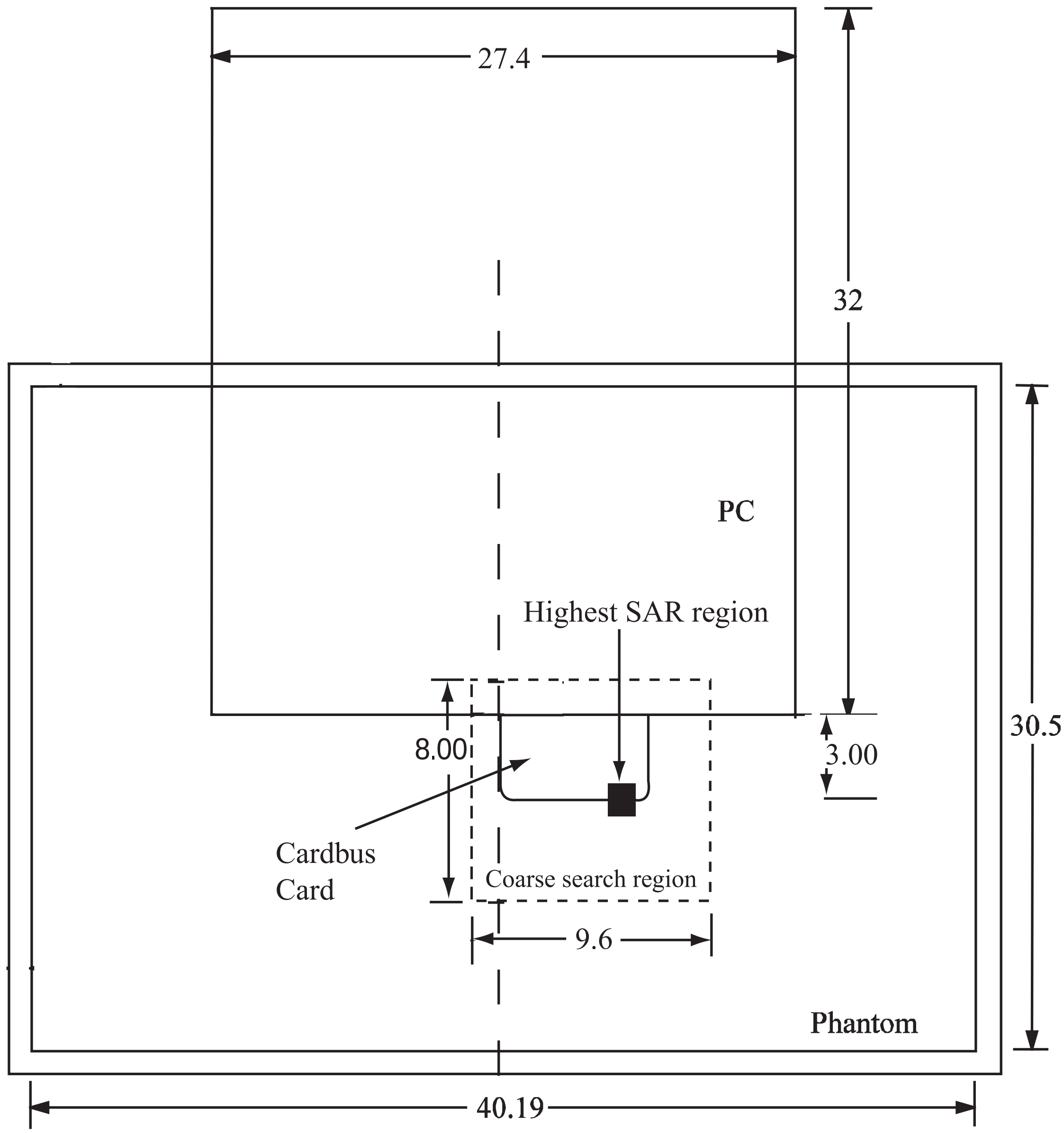

Fig. 14. Illustration of the peak SAR location with respect to the phantom and the Proxim Europe B.V. Model 8460-05 Cardbus Card for the **Above-lap position**. All dimensions are in cm.

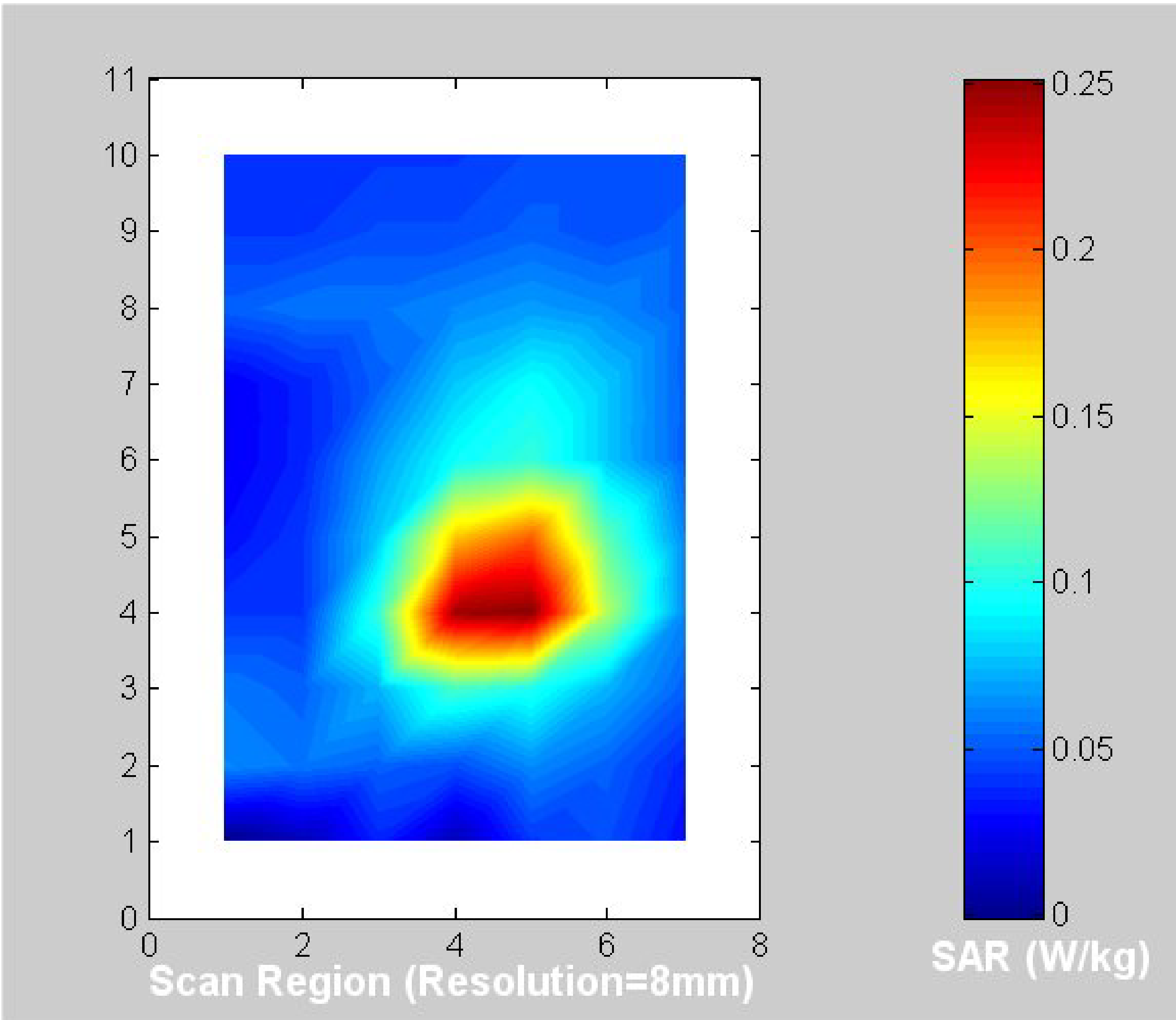

(a) 5.26 GHz base mode (see Table 7 for the peak 1-g SAR).

Fig. 15. Coarse scans for the SAR measurements for the **End-on position** of the Proxim Europe B.V. Model 8460-05 Cardbus Card touching the base of the flat phantom.

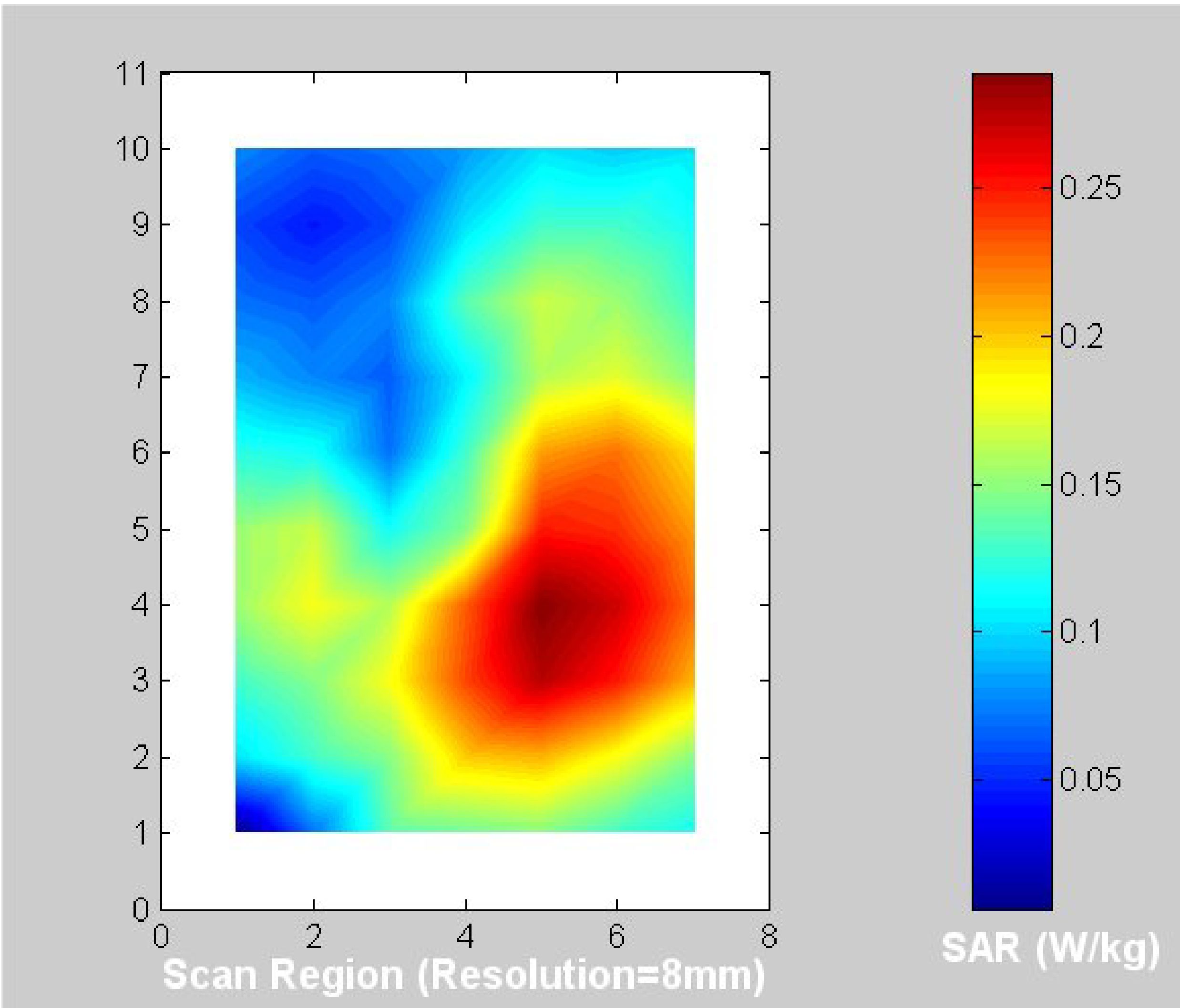

(b) 5.785 GHz base mode (see Table 8 for the peak 1-g SAR).

Fig. 15. Coarse scans for the SAR measurements for the **End-on position** of the Proxim Europe B.V. Model 8460-05 Cardbus Card touching the base of the flat phantom

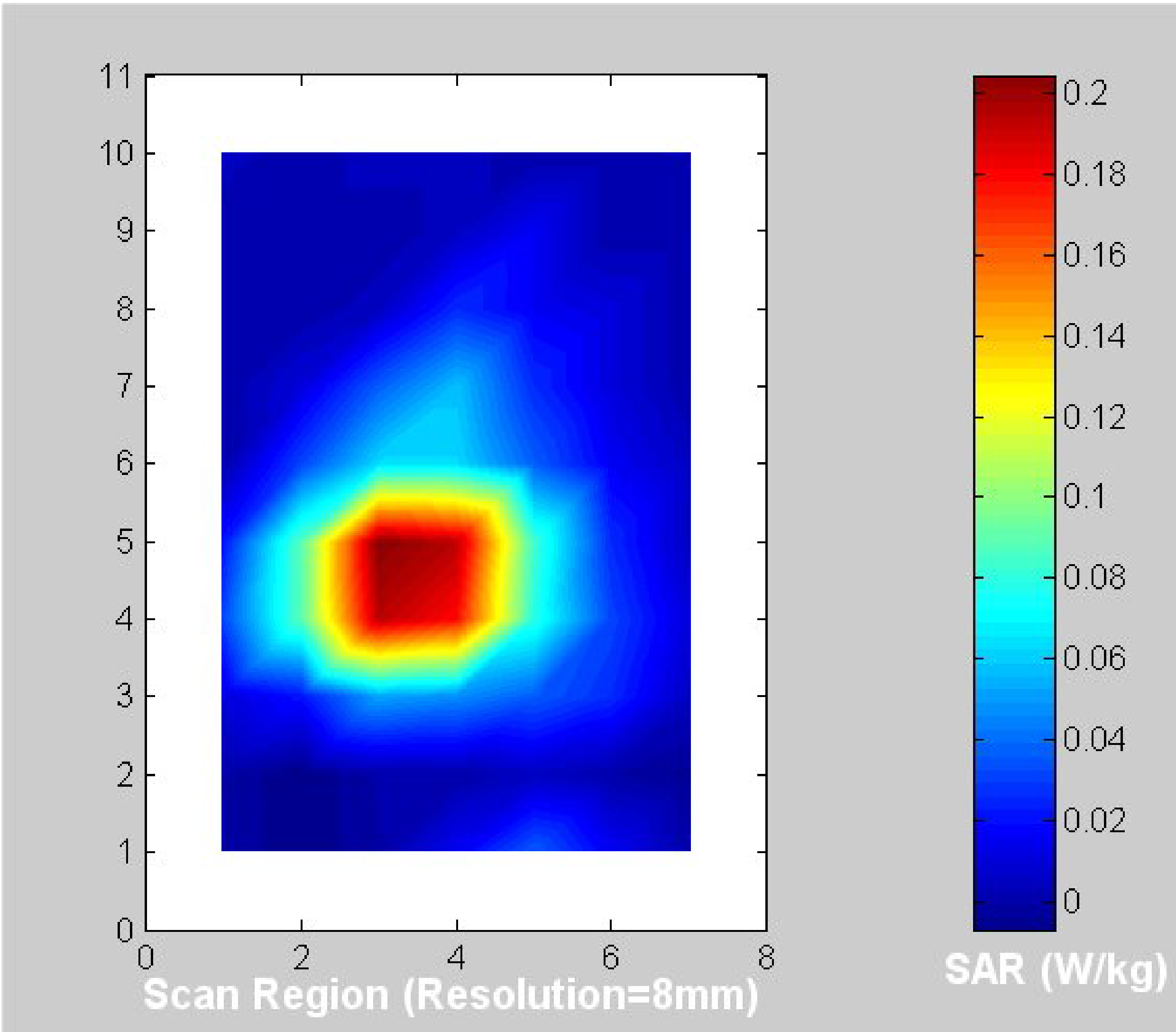

(c) 5.29 GHz turbo mode (see Table 9 for the peak 1-g SAR).

Fig. 15. Coarse scans for the SAR measurements for the **End-on position** of the Proxim Europe B.V. Model 8460-05 Cardbus Card touching the base of the flat phantom.

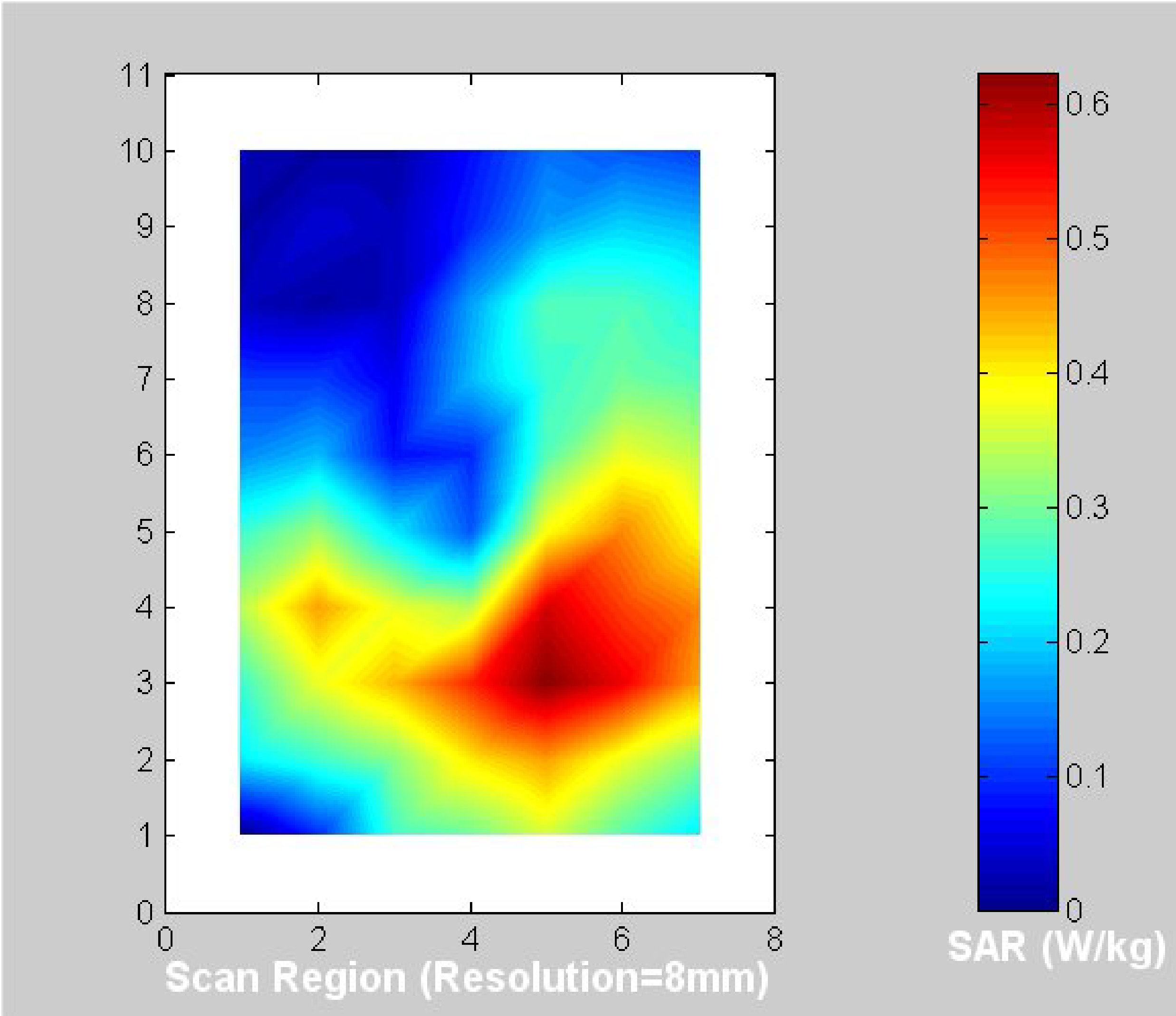

(d) 5.800 GHz turbo mode (see Table 10 for the peak 1-g SAR).

Fig. 15. Coarse scans for the SAR measurements for the **End-on position** of the Proxim Europe B.V. Model 8460-05 Cardbus Card touching the base of the flat phantom.

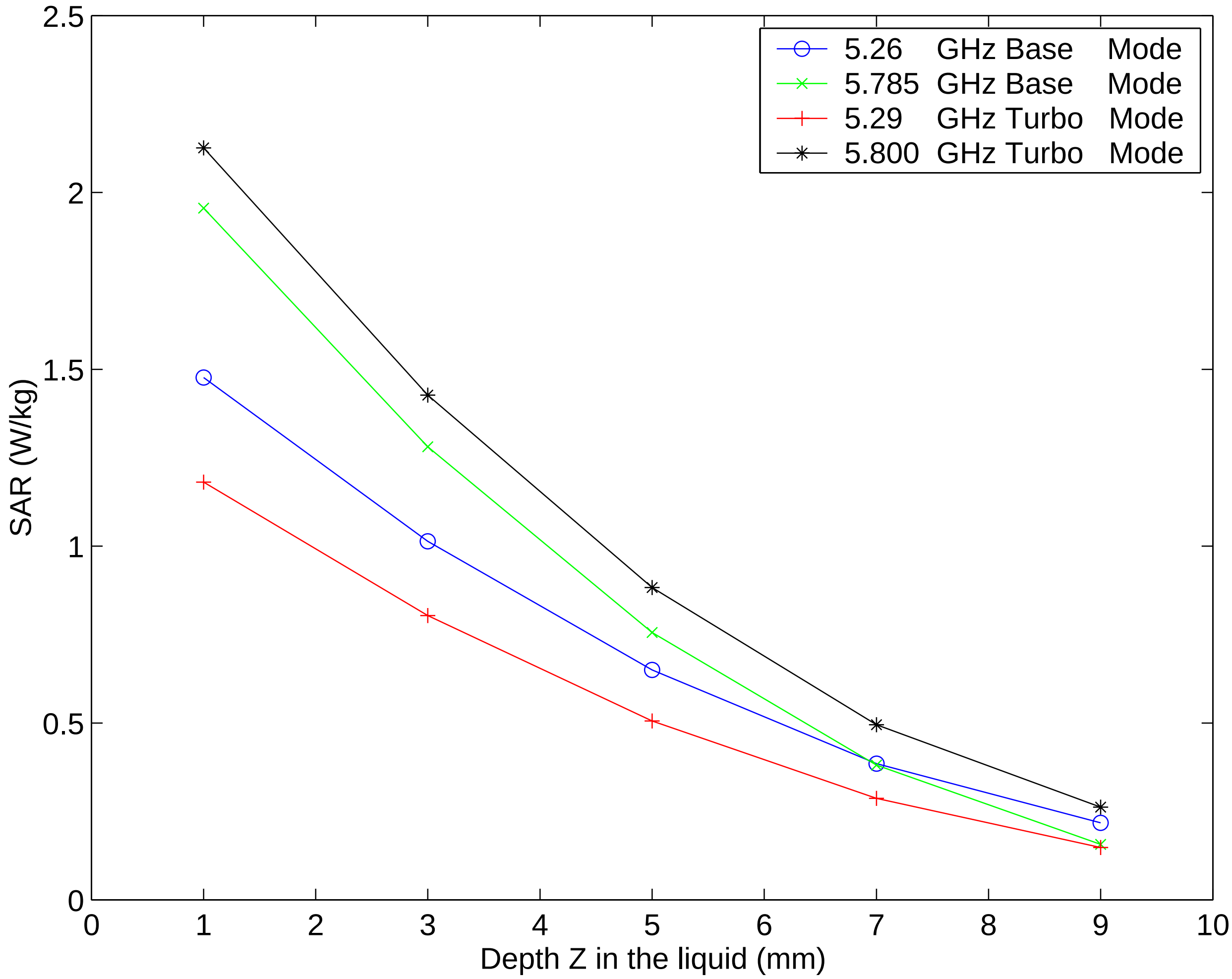

Fig. 16. Plot of the SAR variations as a function of depth Z in the liquid for locations of highest SAR (from Tables 3-6 -- Above-lap position) for the Proxim Europe B.V. Model 8460-05 Cardbus Card.

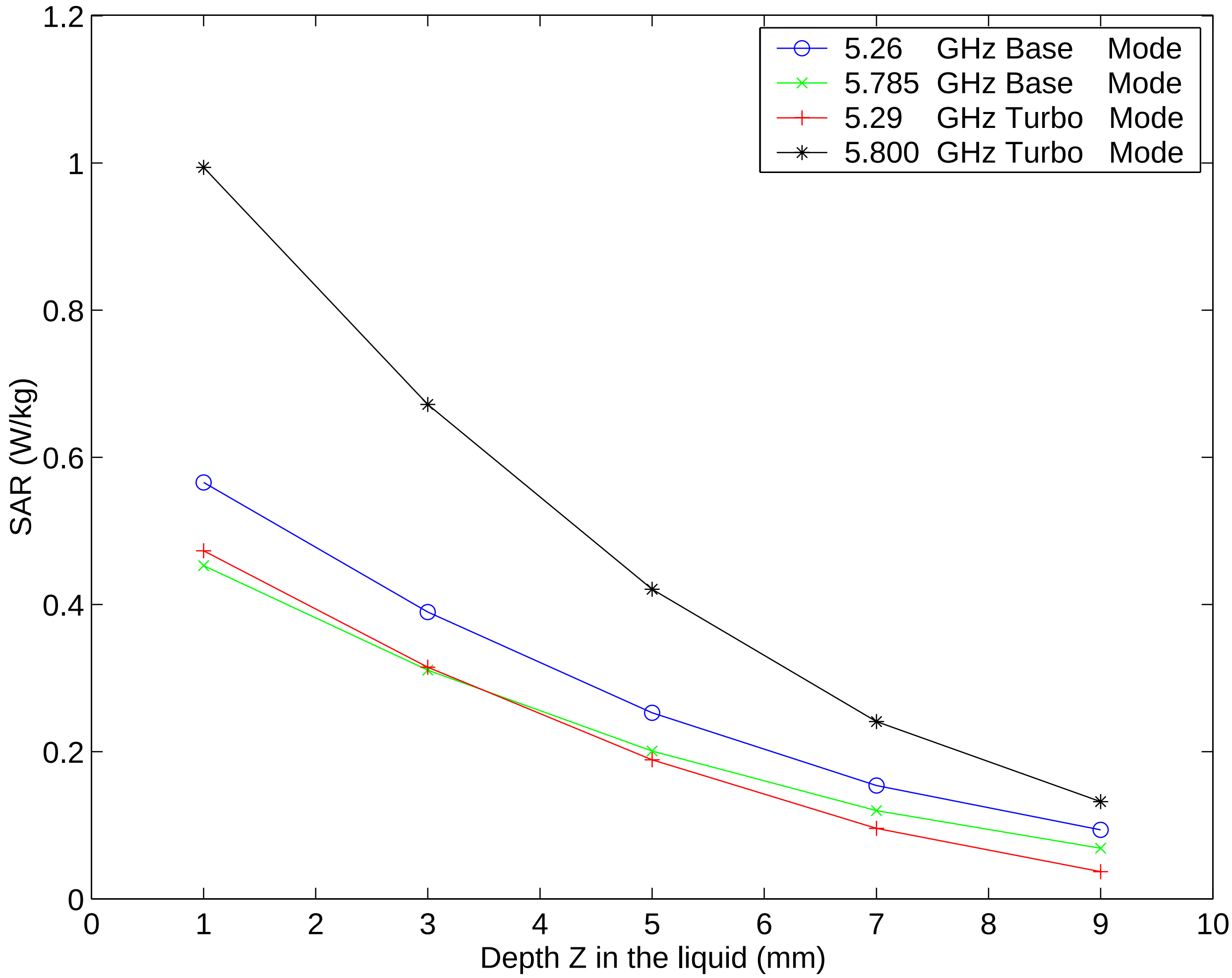

Fig. 17. Plot of the SAR variations as a function of depth Z in the liquid for locations of highest SAR (from Tables 7-10 -- End-on position) for the Proxim Europe B.V. Model 8460-05 Cardbus Card.

APPENDIX B

SAR System Verification for December 21, 22, 2002

The measured SAR distribution for the peak 1-g SAR region using a dipole at 1900 MHz

For December 21, 2002 - The dipole SAR Plot

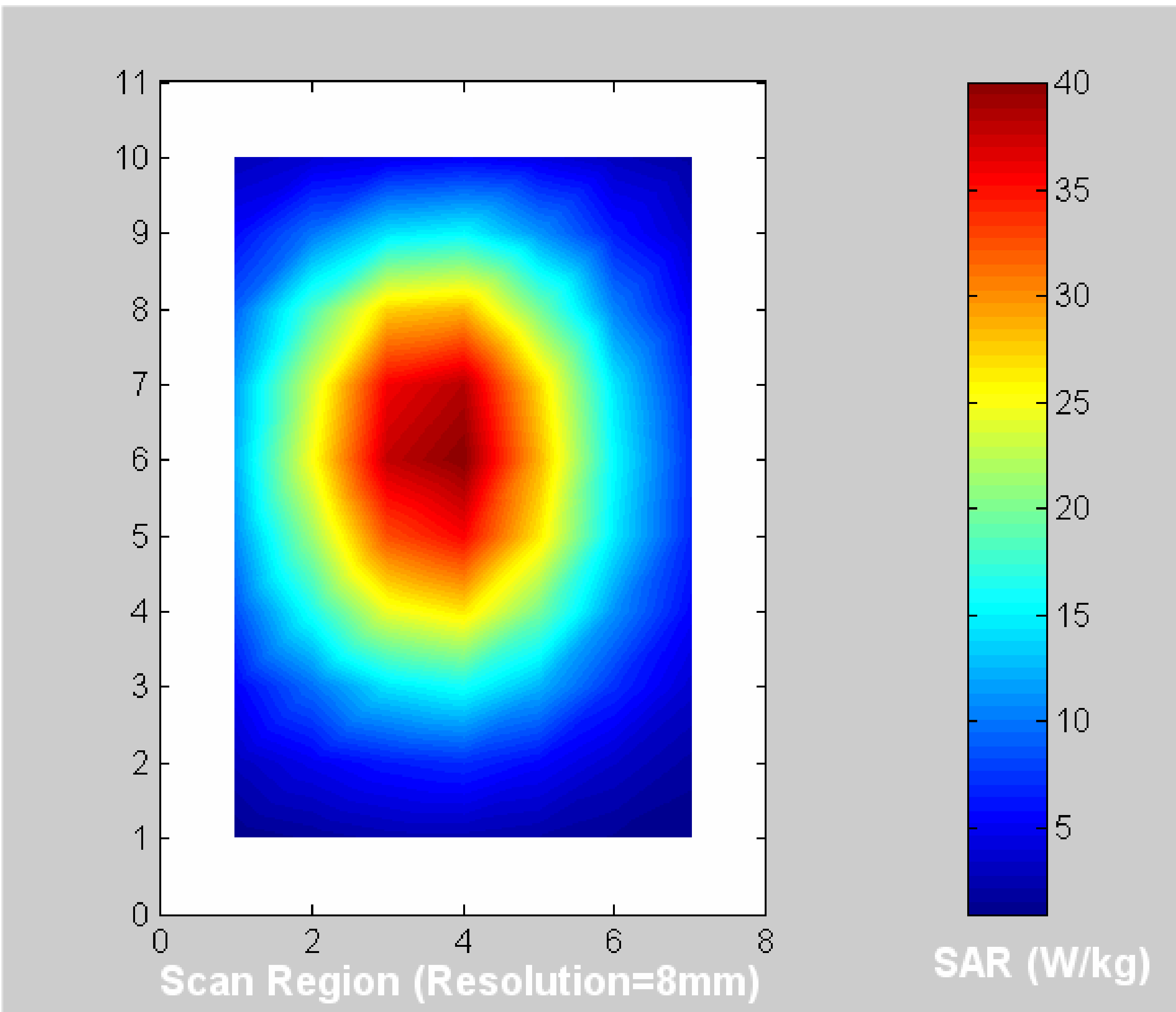

1-g SAR = 36.001 W/kg

a. At depth of 1 mm

54.335	57.747	59.189	59.096	57.129
54.805	57.773	59.157	59.016	56.887
54.178	57.438	58.686	58.559	56.448
53.269	56.050	57.434	57.255	55.186
51.768	54.394	55.558	55.277	53.081

b. At depth of 3 mm

42.888	45.388	46.402	46.311	44.872
43.205	45.424	46.395	46.253	44.706
42.734	45.111	46.061	45.924	44.386
42.008	44.092	45.096	44.903	43.413
40.866	42.809	43.630	43.427	41.829

c. At depth of 5 mm

33.193	34.942	35.611	35.525	34.512
33.385	34.983	35.621	35.484	34.409
33.050	34.708	35.405	35.264	34.188
32.477	33.985	34.679	34.487	33.459
31.632	33.013	33.560	33.415	32.307

d. At depth of 7 mm

25.252	26.410	26.815	26.738	26.049
25.344	26.448	26.837	26.712	25.996
25.124	26.228	26.719	26.580	25.855
24.676	25.728	26.182	26.008	25.323
24.065	25.005	25.348	25.241	24.515

e. At depth of 9 mm

19.063	19.791	20.015	19.949	19.483
19.081	19.820	20.041	19.934	19.467
18.958	19.671	20.001	19.871	19.385
18.604	19.323	19.604	19.465	19.005
18.165	18.786	18.994	18.905	18.452

For December 22, 2002 - The Dipole SAR Plot

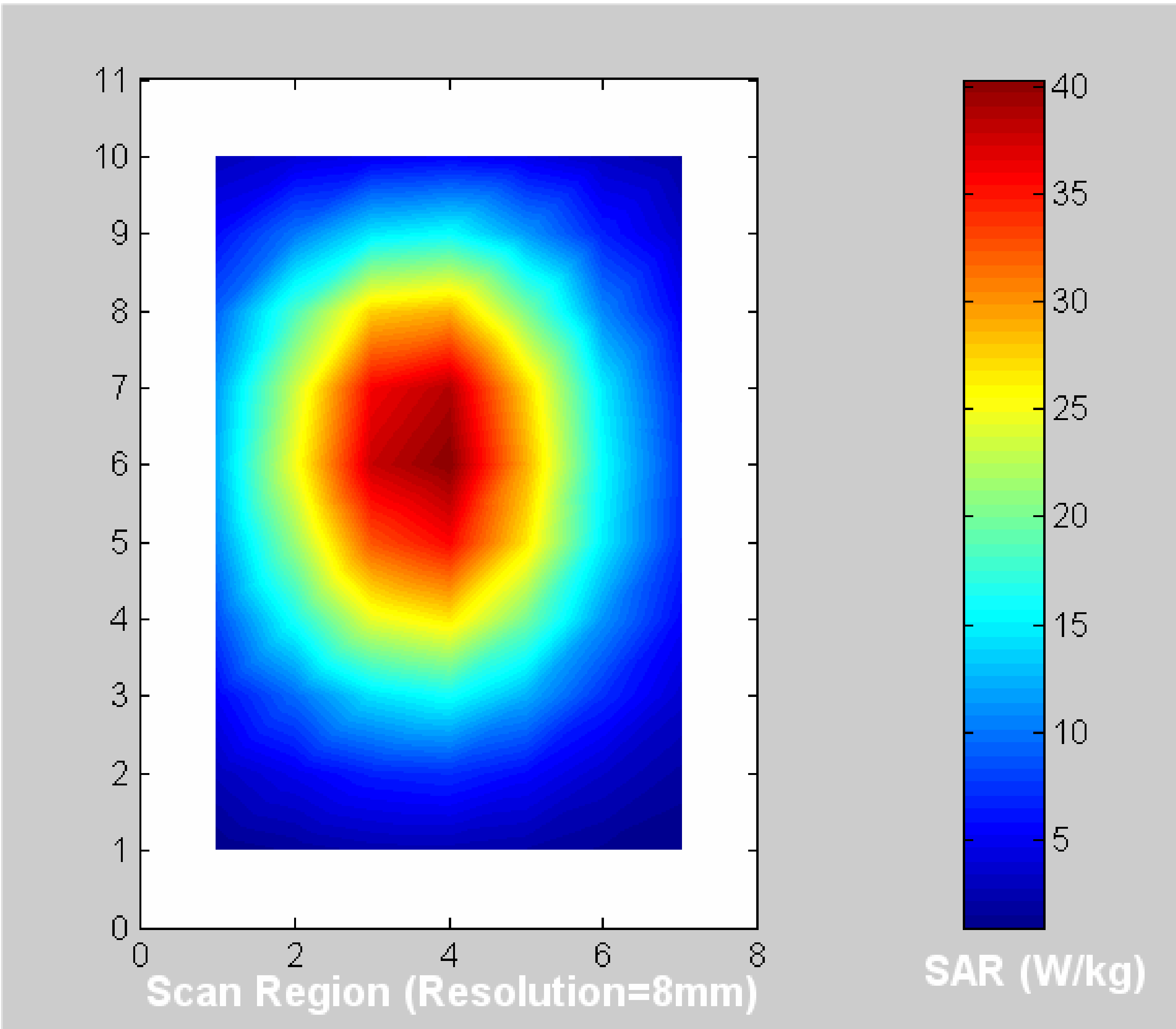

1-g SAR = 36.165 W/kg

a. At depth of 1 mm

53.328	56.674	58.326	58.272	56.539
54.359	57.584	59.222	58.983	57.203
54.382	57.607	59.208	59.116	57.165
53.904	57.037	58.460	58.281	56.280
52.978	55.718	56.990	56.700	54.687

b. At depth of 3 mm

42.041	44.500	45.680	45.633	44.329
42.842	45.220	46.346	46.190	44.874
42.881	45.226	46.384	46.302	44.866
42.528	44.810	45.828	45.671	44.226
41.772	43.804	44.748	44.511	43.013

c. At depth of 5 mm

32.487	34.213	35.013	34.965	34.016
33.097	34.773	35.492	35.398	34.459
33.144	34.771	35.570	35.492	34.478
32.893	34.484	35.174	35.040	34.037
32.290	33.735	34.403	34.216	33.149

d. At depth of 7 mm

24.665	25.814	26.324	26.268	25.600
25.123	26.243	26.663	26.607	25.957
25.171	26.242	26.767	26.687	25.999
25.000	26.059	26.498	26.387	25.713
24.529	25.512	25.956	25.815	25.096

e. At depth of 9 mm

18.575	19.303	19.613	19.544	19.082
18.920	19.629	19.857	19.816	19.368
18.964	19.640	19.975	19.885	19.431
18.849	19.534	19.801	19.713	19.253
18.492	19.134	19.406	19.308	18.852

APPENDIX C

Uncertainty Analysis

The uncertainty analysis of the University of Utah SAR Measurement System is given in Table A.1. Several of the numbers on tolerances are obtained by following procedures similar to those detailed in [8], while others have been obtained using methods suggested in [4].

Table B.1. Uncertainty analysis of the University of Utah SAR Measurement System.

Uncertainty Component	Tolerance ± %	Prob. Dist.	Div.	C_i 1-g	1-g u_i ± %
Measurement System					
Probe calibration	2.0	N	1	1	2.0
Axial istropy	4.0	R	√3	$(1\text{-}cp)^{1/2}$	1.6
Hemispherical isotropy	5.5	R	√3	$\sqrt{c_p}$	0.0
Boundary effect	0.8	R	√3	1	0.5
Linearity	3.0	R	√3	1	1.7
System detection limits	1.0	R	√3	1	0.6
Readout electronics	1.0	N	1	1	1.0
Response time	0.0	R	√3	1	0.0
Integration time	0.5	R	√3	1	0.3
RF ambient conditions	0	R	√3	1	0
Probe positioner mechanical tolerance	0.5	R	√3	1	0.3
Probe positioning with respect to phantom shell	2.0	R	√3	1	1.2
Extrapolation, interpolation, and integration algorithms for max. SAR evaluation	5.0	R	√3	1	2.9
Test Sample Related					
Test sample positioning	3	R	√3	1	1.7
Device holder uncertainty	3	R	√3	1	1.7
Output power variation - SAR drift measurement	5	R	√3	1	2.9
Phantom and Tissue Parameters					
Phantom uncertainty - shell thickness tolerance	10.0	R	√3	1	5.8
Liquid conductivity - deviation from target values	0.4	R	√3	0.7	0.2
Liquid conductivity - measurement uncertainty	1.5	R	√3	0.7	0.6
Liquid permitivity - deviation from target values	0.8	R	√3	0.6	0.3
Liquid permittivity - measurement uncertainty	3.5	R	√3	0.6	1.2
Combined Standard Uncertainty		RSS			8.3
Expanded Uncertainty (95% Confidence Level)					16.6